Hindawi
Shock and Vibration
Volume 2024, Article ID 5213904, 12 pages
https://doi.org/10.1155/2024/5213904

Research Article

Analysis of Vibration Transmission Path in Packaging System and Design of Teaching Experiment

Meilin Gong[1] **and Cong Lin**[2]

[1]*Administrative Office of Discipline Construction and Graduate Program, Jinan University, Zhuhai 519070, China*
[2]*Packaging Engineering Institute, Jinan University, Zhuhai 519070, China*

Correspondence should be addressed to Meilin Gong; gongml@jnu.edu.cn

Received 6 December 2023; Revised 26 December 2023; Accepted 4 January 2024; Published 22 January 2024

Academic Editor: E. Jiaqiang

It is essential for realizing the most suitable product buffer packaging design to quantify the vibration transmission characteristics of the product packaging system. The experiment system for the vibration transmission path of protective packaging is designed in this paper. The practical system is used to analyze the vibration transfer path of the product packaging system and identify the critical transfer path. The concepts of the cushions' contribution rate and the cushions' weighted contribution rate are introduced. The product cushioning based on the weighted equal contribution rate of the cushions is proposed. It has been verified by experiments that the system can accurately identify the transfer path with the weighted contribution rate of the cushions as a reference for the design of product buffer packaging, which improves the utilization rate of buffer packaging materials and reduces the cost of packaging materials. The weighted equal contribution rates of buffer pads 1, 2, 3, and 4 are 40%, 27%, 22%, and 11%, respectively. For the needs of experiment teaching, the teaching content based on the protective packaging transfer path testing system is designed, which provides a reference for the practical education of the packaging specialty.

1. Introduction

With the rapid development of the logistics and transportation industry, the use of the foam to cushion and products protection is increasing with a series of economic and ecological problems. To respond to the call for plastic restriction [1], courier packaging reduction [2] has become an urgent problem in the packaging industry. At present, the cushioning design of products in transportation is usually based on the dynamic cushioning characteristics curve of (DCCC) cushioning materials and the transfer rate curve of material thickness and static stress. The process includes calculating the area and thickness of cushioning materials required for the products, carrying out comprehensive cushioning or local cushioning, and testing the packaging prototypes to verify the cushioning vibration reduction effect. This method is based on the characteristics of cushioning materials based on empirical. The cushioning area of each part is mostly uniformly distributed in the local cushioning, which needs to improve the utilization rate of cushioning materials. The research points of the vibration transmission characteristics (VTC) of product packaging systems [3] under actual environmental excitation have more advantages compared to the DCCC method [4, 5]. The VTC analyzes the critical vibration transmission path of the product and carries out essential buffer design for it. The VTC carries out reduced buffer design for the nonkey vibration transmission path of the product, which makes full use of the buffer materials in each part to reduce the cost of buffer packaging. The transfer path method [6, 7] is an effective tool for VTC analysis. The path can analyze the excitation energy of each excitation source or each transfer path into the target source of the proportion of the overall system vibration energy through the transfer [8].

A number of scholars have studied the dynamic characteristics of product packaging systems [9, 10]. Wang et al.

[11] used the inverse analysis of the dynamical response of coupled product transport systems on the inverse substructuring method, which can optimize the design of cushioning packages. Li et al. [12] analyzed the contribution of each vibration path of the gearbox based on the velocity intervention loss to identify the main transmission path of the gearbox vibration. The vibration test of the gearbox was carried out to verify the correctness of the transmission path model. Fan et al. [13] got the path contribution of fan noise in the converter and transformer noise sources to determine the main contributing paths by the transfer path analysis test. The simulations were performed to verify the experimental results.

Among the transfer path methods, the advanced transfer path analysis (ATPA) method is widely used in the field of noise and vibration control due to its experiment simplicity, no need for load identification, and theoretical decoupling between transfer paths. Magrans and Guasch [14] applied the ATPA methodology to identify the contribution of antennas and structural panels to the interior noise of the bus. The modifications were made to reduce the interior noise level at a given location based on the contribution from some structural elements of the bogie or the engine. Aragones et al. [15] used the ATPA method to the rectangular body model and developed a numerical model of the rectangular box based on finite elements, which reconstructed the working condition signals through a direct transfer function. It presented a good agreement between measured and numerical results, which provided a reference for the numerical modeling study of the ATPA method. Wang and Zhu [16] further developed the predictive capabilities of the ATPA by extending 2 path-blocking techniques. It used easily measurable variables from the original system to predict the response of path-blocked systems to finite element models of continuous systems, which can predict structural vibration transfer after path modification. Liao et al. [17] investigated the vibration transfer characteristics of coupled systems with Neumann series based on the higher transfer path method, which can further expand the application scope of the method. Malkoun et al. [18] developed a method for separating track and vehicle rolling noise based on ATPA, which obtained the separation of track and vehicle noise for a specific rolling stock on a specific track. It can realize the separation of track and vehicle noise for different types of rolling stock on different types of tracks.

The establishment of the universally applicable experimental system for the transfer path of product packaging components is necessary for product packaging design. It is necessary to establish a universally applicable experiment system for product packaging transmission path for product packaging design. This paper designs a protective packaging transmission path experimental system, which can analyze the contribution of each vibration transmission path for any locally buffered product packaging system. Based on the design principle of weighted equal contribution rate of buffer pads, the experiment system provides a scientific basis for the reduction design of buffer packaging.

2. Packaging Vibration Design Considerations and Requirements

Design of teaching experiment system design for transmission path and process of protective packaging of electrical products are based on the packaging design considerations which are listed as follows.

(1) The attributes of the product itself: the allowable brittleness value, shape, size, weight, volume, center of gravity, and quantity of the product.

(2) Environmental conditions during the circulation process, such as transportation intervals, transportation methods, loading and unloading times, equivalent drop height, impact direction, climatic conditions, and storage conditions

(3) Characteristics of packaging materials

(4) The structure, shape, material, and strength of the outer packaging container

(5) Characteristics of sealing materials

(6) Packaging craftsmanship

(7) Other packaging methods, such as moisture-proof, waterproof, rustproof, and dustproof.

The requirements for packaging design are given in Figure 1.

3. Design of Teaching Experiment System Design for Transmission Path and Process of Protective Packaging

3.1. Experiment System Devices and Functions. Figure 2 shows the protective packaging transfer path experiment system components, which consist of the computer-side (data processing system), the data acquisition system, and the auxiliary test system. The data processing system includes DASP V11 (data acquisition and signal processing) and MATLAB software. The data acquisition system is made up of the data acquisition instruments, the force hammer, and the acceleration sensor. The auxiliary test system consists of the hanger and the additional mass piece.

Figure 3 shows the experiment system principle chart. The hanger in the auxiliary test system lifts the product packaging system and puts it in a free suspension. The additional mass piece is used to assist in signal acquisition. The data acquisition system adopts a single-input multiple-output test method, in which the excitation signal is given by the force hammer excitation and the acceleration response signal is collected by the acceleration sensor. The outputs of both the force hammer and the acceleration sensor are ICP signals. The INV data signal collector converts the excitation signal and the response signal.

The converted signals were passed to the data processing system for analysis. The computer-side software DASP V11 in the data processing system is used to convert the time domain acceleration signals into frequency domain signals. The frequency domain acceleration signals are processed and analyzed in a program prepared by MATLAB software

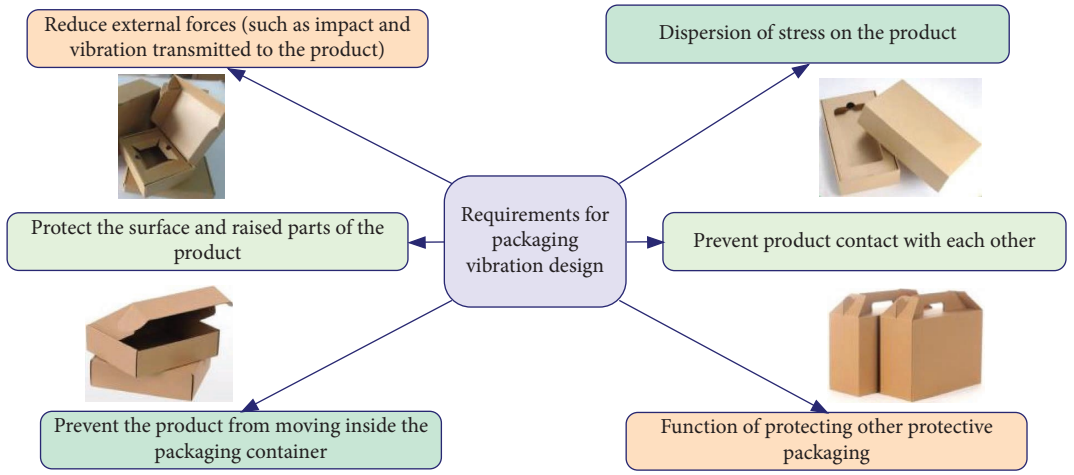

Figure 1: Requirements for packaging vibration design.

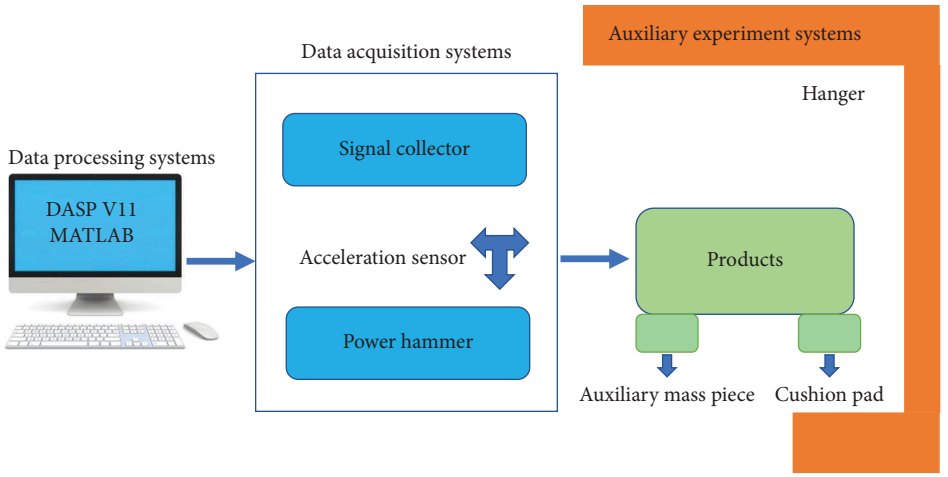

Figure 2: Schematic diagram of the experiment system.

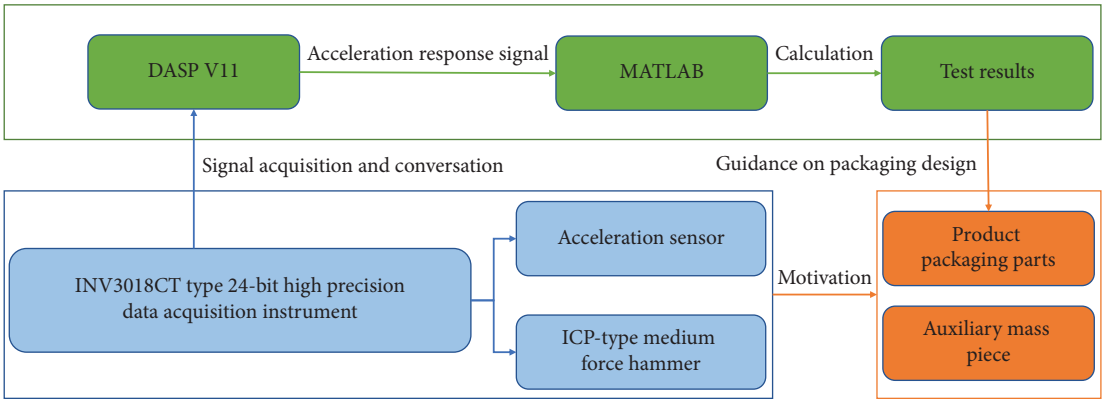

Figure 3: The principle chart of the experiment system.

to obtain the weighted equal contribution rate of each cushion liner, which is used to guide the cushion packaging design.

3.2. The System Work Principles. The experiment system is based on the ATPA of global transmissibility direct transmissibility function advanced transfer path method [19], which

is one of the transfer path methods. The ATPA transfer path method is divided into 2 steps [20]. The first step is to test the overall transfer rate function of the system [21]. The second step is to obtain the direct transfer rate function by calculating the overall transfer rate function and then perform the vibration transfer path contribution analysis for each path [22].

The overall transfer rate function global transmissibility function (GTF) represents the ratio of the response signal of target point j to the response signal of subsystem i when the excitation is applied at the point i [22]. The direct transmissibility function (DTF) represents the ratio of the response signal of target point j caused by subsystem i only to the response signal of that subsystem i when excitation is applied at the point i. The direct transfer function represents the direct transfer capability from subsystem i to subsystem j when the other subsystems are shielded. In the transportation process, the coupling excitation of road and vehicle is transferred to the product. The vibration of key components is transmitted to the bottom plate of the car through the padding of the product packaging. The protection of critical components is crucial, which are the most easily damaged components in a product. The product packaging system is divided into a vital component subsystem and a cushion liner subsystem. The advanced transfer path method is applied to study the vibration impact of each part of the cushion liner on the product. The DTF is used to quantify the vibration transfer capability from a particular cushion liner subsystem to the critical component of the product.

For the product packaging system, the vibration response s_o of the product critical component subsystem is equal to the vector superposition of the input cushion system excitation signal s_i and the direct transfer function T_{io}^D multiplied from each cushion subsystem to the essential component subsystem. The theoretical equation can be expressed as follows:

$$s_o = \sum T_{io}^D s_i. \tag{1}$$

The product packaging system has n subsystems. It is assumed that the force hammer acts on the cushion liner subsystem i; the product key element subsystem is j ($i \neq j$). Point e refers to the path point of a subsystem and the response at point j is equal to the sum of the response components transmitted directly to point j from all path points as given in the following equation:

$$s_j = \sum_{e=1,e\neq j}^{n} s_{\mathrm{kj}}^D. \tag{2}$$

s_{ej}^D is the signal component passed directly from point e to point j. s_{ej}^D is equal to the work response signal at point e multiplied by the direct transfer rate function from point e to point j as listed in the following equation:

$$s_{ej}^D = s_e \times T_{ej}^D. \tag{3}$$

According to the definition of the overall transfer rate function, the overall transfer rate function from point i to point e is equal to the ratio of the response signal at point e to the response signal at end i as displayed in the following equation:

$$s_e = s_i \times T_{ik}^G. \tag{4}$$

T_{ie}^G is the overall transfer rate function from point i to point e. Substituting equations (2) and (3) into equation (1) yields the following equation:

$$s_j = \sum_{e=1,e\neq j}^{n} s_i \times T_{\mathrm{ie}}^G T_{\mathrm{ej}}^D. \tag{5}$$

Equation (5) can be rewritten as follows:

$$s_j = s_i \times T_{ij}^G. \tag{6}$$

Substituting equations (6) into equation(5) yields the following equation:

$$T_{ij}^G = \sum_{e=1,e\neq j}^{n} T_{ie}^G T_{ej}^D, \quad i \neq j. \tag{7}$$

Therefore, the overall transfer rate function matrix is related to the direct transfer rate matrix as given in the following equation:

$$\begin{bmatrix} T_{11}^G & T_{12}^G & \cdots & T_{1n}^G \\ T_{21}^G & T_{22}^G & \cdots & T_{2n}^G \\ \vdots & \vdots & \ddots & \vdots \\ T_{n1}^G & T_{n2}^G & \cdots & T_{nn}^G \end{bmatrix} \begin{bmatrix} T_{1j}^D \\ T_{2j}^D \\ \vdots \\ T_{nj}^D \end{bmatrix} = \begin{bmatrix} T_{1j}^G \\ T_{2j}^G \\ \vdots \\ T_{nj}^G \end{bmatrix}. \tag{8}$$

Equation (9) is the vibration contribution of each cushion liner to the critical components of the product s_o^i.

$$s_o^i = s_i T_{io}^D. \tag{9}$$

The frequency point where the critical components of a product are most likely to be damaged is at the resonance peak. The vibration contribution rate of the cushion pads at the resonance peak is significant.

The concept of equal contribution rate of cushion pads (ECP) is introduced and defined as the ratio of the contribution of the i cushion pad to the resonance peak of the critical component s_{op}^i to the peak vibration response s_{op} of the crucial component under the external environmental excitation as shown in the following equation:

$$\mathrm{ECP} = \frac{s_{op}^i}{s_{op}}. \tag{10}$$

There are multiple resonance areas during vibration. The analysis is performed at the most dominant resonance peak if the peak of each resonance area differs significantly. The study is weighted if the height of multiple resonance areas does not vary greatly.

The weighted equal contribution rate of cushion pads (WECP) is defined as the superposition of the cushion equal contribution rate of the i cushion pad at the j resonance peak multiplied by the ratio of the j resonance peak to the sum of all resonance peaks as shown in the following equation:

$$\mathrm{WECP} = \sum_{i=1,j=1}^{n} \mathrm{ECP}_i \times \frac{s_{op_j}}{\sum s_{op_j}}. \quad (11)$$

The cushion liner's weighted contribution rate is the cushion design evaluation basis. According to the weighted contribution rate of the cushion liner, the key or nonkey protection of the cushion liner is carried out at each position of the product. The larger the weighted contribution rate of the cushion liner, the more protection is needed. The smaller the weighted contribution rate of the cushion liner, the less protection is required. The design of cushion liners to protect the product and minimize the cost of cushion packaging can be optimized.

3.3. Experiment System Operation Procedure. The experiment system operation process can be carried out in 6 steps as follows.

(1) Measure the response signals between all subsystems and then compare them to obtain the overall transfer rate function TG. The function includes the overall transfer rate function between the buffer liner subsystems and the overall transfer rate function between the target subsystems.

(2) Calculate the direct transfer rate matrix from the cushion liner subsystem to the target subsystem based on the relationship between the overall transfer rate function and the natural transfer rate

(3) Measure the signals of the cushion liner subsystem and the target subsystem under the actual working conditions

(4) Based on the direct transfer rate from the cushion liner subsystem to the crucial element subsystem and the excitation signal of the cushion liner subsystem under the actual working conditions, the response of the critical element subsystem is reconstructed. The reconstructed response signal of the essential element subsystem is fitted with the measured movement of the subsystem to verify the correctness.

(5) The equal contribution rate and weighted similar contribution rate of each cushion liner are calculated

(6) Perform cushion packaging design analysis based on the weighted equal contribution rate of the cushion liner.

Figure 4 shows the experiment steps.

3.4. Experiment Subjects. The actual product packaging system was tested with the experiment system to verify effectiveness in order to verify the feasibility of the experimental system. The computer mainframe is a typical electronic product with internal complexly connected components. Buffer protection is needed to avoid damage to its internal components in transport. The computer mainframe is the test object and the computer motherboard is the critical protection component. The main parts of the computer mainframe and selected key components are listed in Table 1.

The dimensional parameters are given in Table 2. The preliminary design of the buffer package of the product packaging system was carried out to ensure the rationality of the initial setup.

4 buffer corner pads of the same size were used to buffer and protect the computer mainframe, and the buffer material was foamed polyethylene with the density of 26 kg/m^3. The 4 cushion pads are numbered 1, 2, 3, and 4 in clockwise order from a corner near the computer motherboard, which is displayed in Figure 5.

3.5. Experiment Steps. Table 3 lists the experiment equipment and apparatus. The product packaging system is first lifted with a hanger to make it free-hanging during the experiment. The auxiliary mass piece is glued to the bottom of the cushion liner to keep the overall horizontal state.

Figure 6 shows the computer mainframe components and the selected key components. The acceleration sensor is installed on the auxiliary mass piece of each cushion liner after determining the location of the measurement points. The acceleration sensor is installed on the computer motherboard.

Figure 7 shows the computer motherboard measurement points. The force hammer is installed with the acceleration sensor to the channel of the data acquisition instrument. The data acquisition instrument is connected with the computer. Ensure that the device is properly connected and then perform the test. Each measurement point was struck 7 times and sampled 7 times accordingly to reduce the error of the hammer. The 7 samplings data were averaged as a set of data. Due to the interference of noise in the signal during the experiment, it is necessary to check the measurement data, such as poor coherence of the measurement points. The experiment should continue until the measurement point of the frequency response function has better coherence and can be used. When the collected data are correct, the measured signals are averaged and windowed, which is input into the program prepared by MATLAB for the analysis of the vibration contribution of each cushion liner. The road transportation is the primary mode of transportation for the computer mainframe. The ASTM standard truck spectrum was selected as the simulated excitation signal for testing to obtain the measured vibration acceleration response of the computer mainframe under simulated excitation. The movements of the 4 cushion pads input under simulated excitation were multiplied and superimposed with the direct transfer rate function to obtain the fitted response values of the computer motherboard.

3.6. Experiment Teaching Applications of the Laboratory. The experiment content revolves around cushioning reduction design for express packaging products. The instructor teacher first explains the experiment principles and

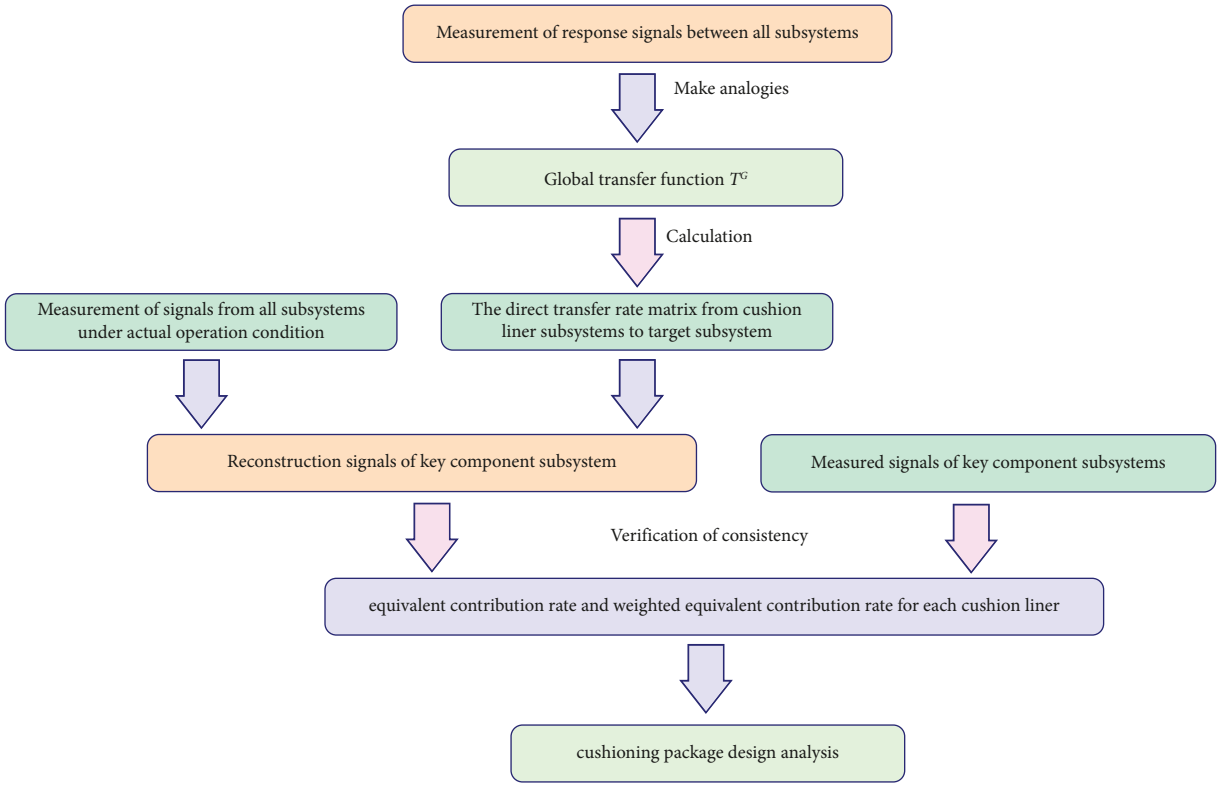

Figure 4: Experiment steps.

Table 1: Computer mainframe components and selected key components.

Computer mainframe components	Selected key components
Power source	Computer motherboard
Display card	Hard disk
Computer motherboard	—
Hard disk	—
Fan	—

Table 2: Dimensions of experimental objects.

Materials	Length (mm)	Width (mm)	Height (mm)
Computer mainframe	380	350	160
EPE cushioning pads	110	60	30
Auxiliary mass piece	100	100	5

data analysis and processing and then gives an introduction to the experiment system and experiment demonstration. The students must master the empirical system principle, operation specification, and data processing method. On this basis, the students work in groups to select commonly used electrical products, analyze the current product packaging design, and put forward suggestions for reducing the amount of packaging in response to the shortcomings of the product design.

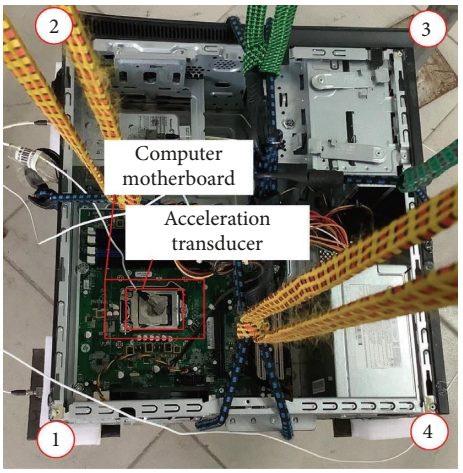

Figure 5: Four buffer corner pads layout arrangement.

The students apply the experiment system to analyze the vibration transmission characteristics of the product packaging system and calculate the cushion contribution rate and the weighted contribution rate of the cushion liner. The helpful report will be written to compare the vibration response of critical components before and after the optimization and the cost of cushioning materials. In addition,

Table 3: Experiment apparatus.

Equipment name	Model	Sensitivity
Data acquisition system	DASP-V11	—
Single-axis acceleration sensors	333B30/40/50	100–1012 mV/g
ICP-type medium force hammer	INV9313	0.195 mV/N

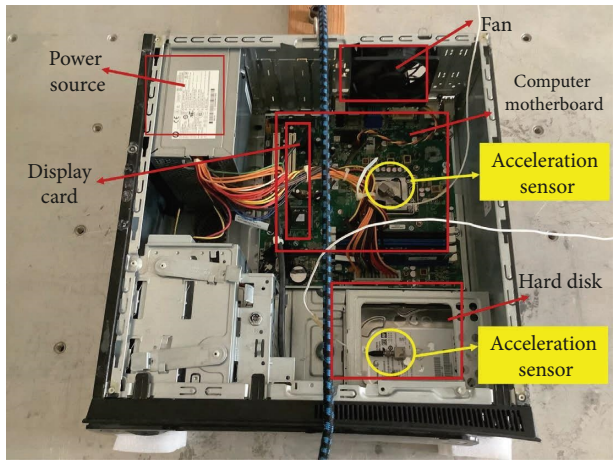

Figure 6: Computer mainframe components and selected key components.

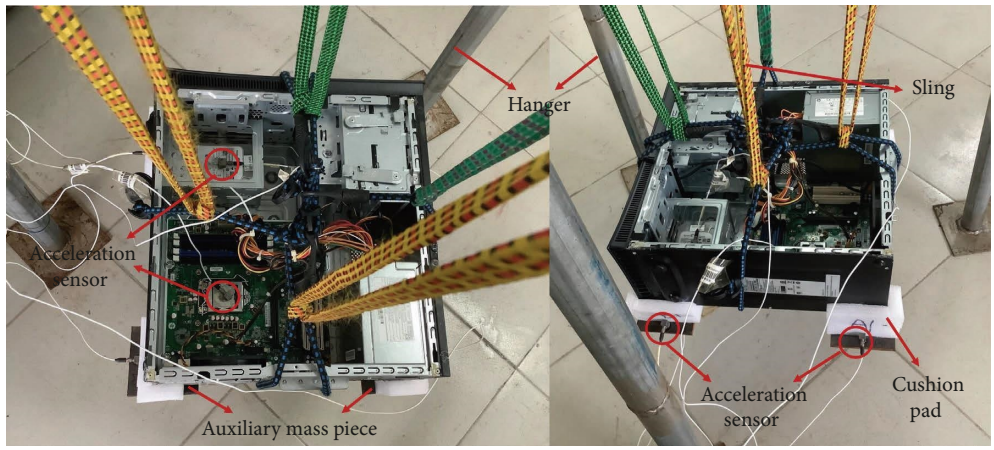

Figure 7: Computer motherboard measurement points.

instructors encourage students to ask questions such as experiment system improvement design, data processing, and other suggestions to increase the buffer design's accuracy. These questions can deepen students' understanding of the practical system and stimulate students' interest in learning about the packaging profession.

4. Results and Discussion

In order to verify the accuracy of this experiment system, the measured acceleration response of the computer motherboard is compared with the fitted acceleration response in the frequency domain. Figure 8 shows the computer motherboard measured response and synthetic response amplitude frequency comparison. The computer motherboard response fitted by the direct transfer rate tested by this experiment system which shows an overall agreement with the measured response with the frequency range from 0 to 100 Hz. Each prominent resonance peak corresponds to one another which indicated the accuracy of this practical test system. The fitted response is slightly larger than the measured response, which made the experimental test results more conservative and reliable. The areas with significant errors between the fitted response and the measured response are located in the second main resonance region, which is also a key consideration in buffer design. The reasons for the errors are the nonlinearity of the actual system and the low coherence function values at individual frequencies.

Figure 9 shows vibration contribution of each cushion liner in the entire frequency band. The excitation of products during transportation is mainly concentrated in

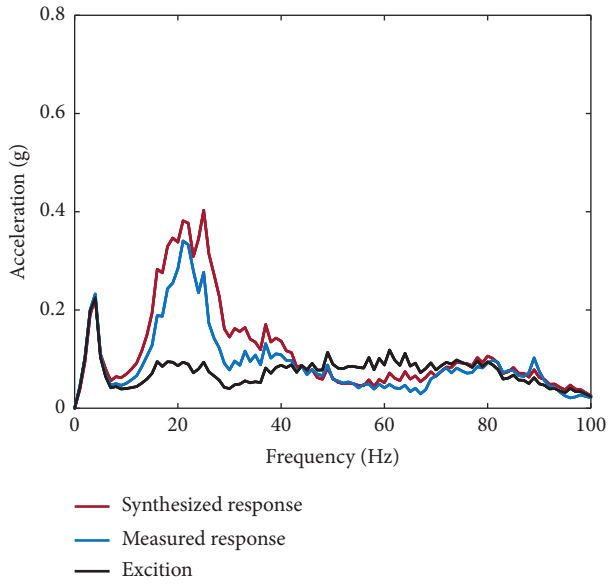

Figure 8: Computer motherboard measured response and synthetic response amplitude frequency comparison.

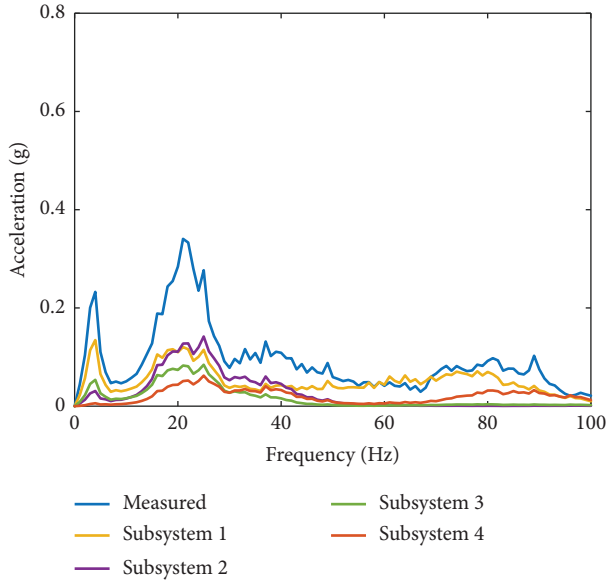

Figure 9: Vibration contribution of each cushion liner in the entire frequency band.

the low-frequency region. More attention is paid to the vibration response in the low-frequency region. In the full frequency range, the computer motherboard has two main resonance regions, namely, 0–10 Hz and 10–30 Hz. In the frequency range of 0–10 Hz from Figure 8, the contribution to the peak vibration response of the computer motherboard is 1, 3, 2, and 4 in descending order. In the frequency range of 10–30 Hz, the contribution to the peak vibration response of the computer motherboard is 2, 1, 3, and 4, respectively.

Figure 10 shows the vibration contribution of each cushion liner in the first primary resonance region. The resonance peak frequency of the first main resonance region is 4 Hz.

The vibration contribution of each cushion liner in the second primary resonance region is shown in Figure 11. The resonance peak frequency of the second main resonance region is 25 Hz. The vibration response of the product is most intense at the resonance peak. The weighted equal contribution rates of buffer pads 1, 2, 3, and 4 are 40%, 27%, 22%, and 11%, respectively.

The vibration contribution of the buffer liner in each main resonance region and the equal contribution rate are listed in Table 4. The cushion packaging design is based on

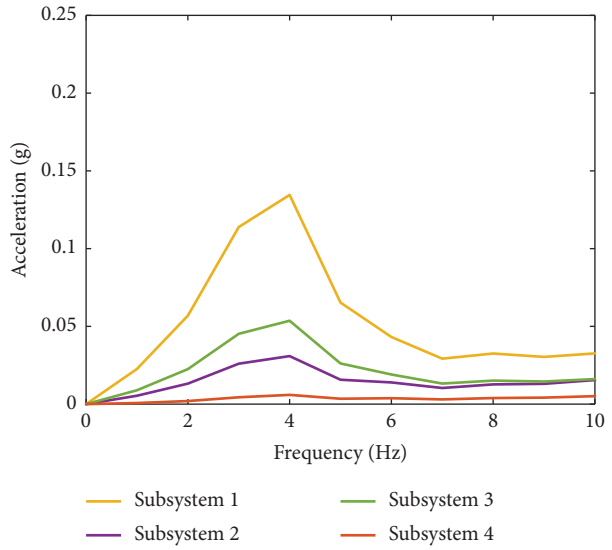

Figure 10: Vibration contribution of each cushion liner in the first primary resonance region.

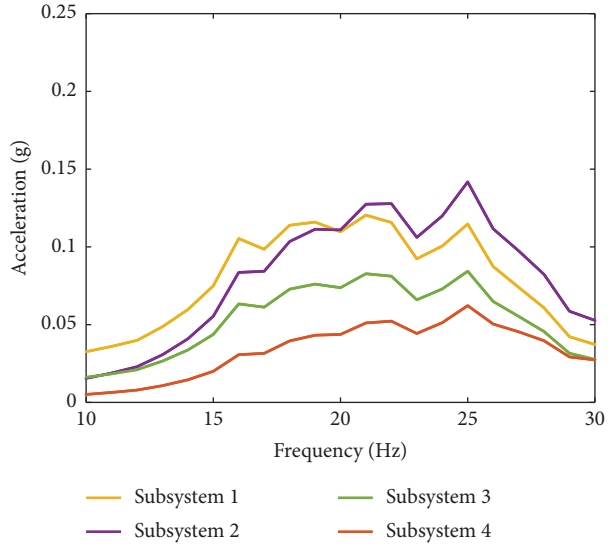

Figure 11: Vibration contribution of each cushion liner in the second primary resonance region.

Table 4: Vibration contribution of cushion liner in each main resonance area and equal contribution rate.

Resonance peak frequency		Computer motherboard	1	2	3	4
First main resonance peak (4 Hz)	Vibration response (g)	0.2226	0.134	0.030	0.0536	0.0060
	The contribution rate of cushion liner etc. (%)		60	13.4	24	2.6
Second main resonance peak (25 Hz)	Vibration response (g)	0.403	0.115	0.142	0.084	0.062
	The contribution rate of cushion liner etc. (%)		28.5	35.2	20.8	15.5
Cushion liner weighted equal contribution rate (%)			40	27	22	11

the weighted equal contribution rate of the cushion liner. The cushion liner design focuses on cushion liners 1, 2, and 3 in order. Cushion liner 4 can be used as a nonfocused liner, which is more scientific and reasonable than the previous way of all cushion liners of the same area.

5. Conclusion

Energy conservation is the theme of scientific research [23–26] and packaging design also follows this principle. With the rapid development of the logistics and transportation industry [27, 28], the reduction of the cost of transportation packaging [29, 30] and product packaging puts forward higher requirements for product cushioning design [31, 32]. The experiment system for the vibration transmission path of protective packaging is designed in this paper with the vibration transfer path of the product packaging system [33]. The experiment system can be used in the teaching applications, which provides a good model for packaging experiment teaching [34]. The conclusions of this paper are as follows.

(1) The concepts of the cushions' contribution rate and the cushions' weighted contribution rate are introduced. The product cushioning based on the weighted equal contribution rate of the cushions is proposed.

(2) The feasibility of the experimental system for vibration transmission characteristics analysis of the product packaging system was verified. The weighted equal contribution rates of buffer pads 1, 2, 3, and 4 are 40%, 27%, 22%, and 11%, respectively.

(3) For the needs of experiment teaching, the teaching content based on the protective packaging transfer path testing system is designed, which provides a reference for the practical education of the packaging specialty.

Nomenclature

n: Subsystems
s_o: Vibration response
s_{ej}^D: Signal component passed directly from point e to point j
T_{ie}^G: Overall transfer rate function from point i to point e
s_o^i: Vibration contribution of each cushion liner to the critical components.
s_{op}: Peak vibration response
s_{op}^i: Contribution of the i cushion pad to the resonance peak of the critical component

Abbreviations

DCCC: Dynamic cushioning characteristics curve
VTC: Vibration transmission characteristics
ATPA: Advanced transfer path analysis
GTF: Global transmissibility function
DTF: Direct transmissibility function
ECP: Equal contribution rate of cushion pads
WECP: Weighted equal contribution rate of cushion pads.

Data Availability

The data used in this study are available from the corresponding author upon reasonable request.

Conflicts of Interest

The authors declare that they have no conflicts of interest regarding the publication of this paper.

Acknowledgments

This work was supported by the Research on Innovation in Scientific Research Management under the Background of "New Liberal Arts" Construction: Strategies and Pathways (no. 12623908) and Model and Path for Building Scientific Research and Innovation Capacity in Science and Engineering at Zhuhai Campus—Taking the School of Intelligent Science and Engineering as an Example (no. 11620803).

References

[1] J. Chu, Y. Zhou, Y. Cai, X. Wang, C. Li, and Q. Liu, "Flows and waste reduction strategies of PE, PP, and PET plastics under plastic limit order in China," *Resources, Conservation and Recycling*, vol. 188, Article ID 106668, 2023.

[2] E. D. Georgakoudis and N. S. Tipi, "An investigation into the issue of overpackaging examining the case of paper packaging," *International Journal of Sustainable Engineering*, vol. 14, no. 4, pp. 590–599, 2021.

[3] Z. W. Wang and Y. B. Zhang, "Dynamic characteristic analysis of refrigerator-truck transport system by using inverse substructure method," *Packaging Technology and Science*, vol. 27, no. 11, pp. 883–900, 2014.

[4] J. Wang, Q. Wang, Z. Sun, L. Lu, and Z. Wang, "Inverse substructuring method for rigidly coupled product transport system based on frequency response function testing probe technique," *Packaging Technology and Science*, vol. 30, no. 8, pp. 373–386, 2017.

[5] J. Wang, X. Hong, Y. Qian, Z. Wang, and L. Lu, "Inverse substructuring method for multi-coordinate coupled product transport system: inverse SUB-structuring method for product transport system," *Packaging Technology and Science*, vol. 27, no. 5, pp. 385–408, 2014.

[6] M. V. Van Der Seijs, D. De Klerk, and D. J. Rixen, "General framework for transfer path analysis: history, theory and classification of techniques," *Mechanical Systems and Signal Processing*, vol. 68-69, pp. 217–244, 2016.

[7] Z. Tang, M. Zan, Z. Zhang, Z. Xu, and E. Xu, "Operational transfer path analysis with regularized total least-squares method," *Journal of Sound and Vibration*, vol. 535, Article ID 117130, 2022.

[8] A. Oktav, Ç Yilmaz, and G. Anlaş, "Transfer path analysis: current practice, trade-offs and consideration of damping," *Mechanical Systems and Signal Processing*, vol. 85, pp. 760–772, 2017.

[9] Z. Liu, Y. Gao, J. Yang et al., "Transfer path analysis and its application to diagnosis for low-frequency transient vibration in the automotive door slamming event," *Measurement*, vol. 183, Article ID 109896, 2021.

[10] D. Lee and J. W. Lee, "Operational transfer path analysis based on deep neural network: numerical validation," *Journal of Mechanical Science and Technology*, vol. 34, no. 3, pp. 1023–1033, 2020.

[11] J. Wang, Q. Wang, L. Lu, and Z. Wang, "Inverse substructuring theory for coupled product transport system based on the dummy masses method," *Packaging Technology and Science*, vol. 29, no. 3, pp. 189–200, 2016.

[12] M. Li, Q. Liu, S. Zhu, S. Ai, W. Chen, and R. Zhu, "Contribution analysis of vibration transmission path of planetary reducer box based on velocity involvement loss," *Journal of Low Frequency Noise, Vibration and Active Control*, vol. 42, no. 1, pp. 39–53, 2023.

[13] L. Fan, J. Zhang, Y. Fan, X. Zhang, and Q. Li, "Study on noise source contribution of converter cabinet based on transfer path analysis test," *Journal of Physics: Conference Series*, vol. 2519, no. 1, Article ID 012034, 2023.

[14] F. X. Magrans and O. Guasch, "The role of the Direct Transfer matrix as a connectivity matrix and application to the Helmholtz equation in 2d: relation to numerical methods and free field radiation example," *Journal of Computational Acoustics*, vol. 13, no. 02, pp. 341–363, 2005.

[15] À. Aragonès, J. Poblet-Puig, K. Arcas, P. V. Rodríguez, F. X. Magrans, and A. Rodríguez-Ferran, "Experimental and numerical study of Advanced Transfer Path Analysis applied to a box prototype," *Mechanical Systems and Signal Processing*, vol. 114, pp. 448–466, 2019.

[16] Z. Wang and P. Zhu, "A system response prediction approach based on global transmissibilities and its relation with transfer path analysis methods," *Applied Acoustics*, vol. 123, pp. 29–46, 2017.

[17] X. Liao, S. Li, S. K. Yang, J. Wang, and Y. Xu, "Advanced component transmission path analysis based on transmissibility matrices and blocked displacements," *Journal of Sound and Vibration*, vol. 437, pp. 242–263, 2018.

[18] A. Malkoun, J. Sapena, and K. Arcas, "Vehicle and rail noise separation method proposal based on transfer path analysis techniques," *21st International Congress on Sound and Vibration*, vol. 5, pp. 4195–4202, 2014.

[19] O. Guasch, "A direct transmissibility formulation for experimental statistical energy analysis with no input power measurements," *Journal of Sound and Vibration*, vol. 330, no. 25, pp. 6223–6236, 2011.

[20] O. Guasch, "Direct transfer functions and path blocking in a discrete mechanical system," *Journal of Sound and Vibration*, vol. 321, no. 3-5, pp. 854–874, 2009.

[21] O. Guasch, C. García, J. Jové, and P. Artís, "Experimental validation of the direct transmissibility approach to classical transfer path analysis on a mechanical setup," *Mechanical Systems and Signal Processing*, vol. 37, no. 1-2, pp. 353–369, 2013.

[22] O. Guasch and F. X. Magrans, "The Global Transfer Direct Transfer method applied to a finite simply supported elastic beam," *Journal of Sound and Vibration*, vol. 276, no. 1-2, pp. 335–359, 2004.

[23] X. Zhao, J. Jiang, H. Zuo, and Z. Mao, "Performance analysis of diesel particulate filter thermoelectric conversion mobile energy storage system under engine conditions of low-speed and light-load," *Energy*, vol. 282, Article ID 128411, 2023.

[24] X. Zhao, J. Jiang, H. Zuo, and G. Jia, "Soot combustion characteristics of oxygen concentration and regeneration temperature effect on continuous pulsation regeneration in diesel particulate filter for heavy-duty truck," *Energy*, vol. 264, Article ID 126265, 2023.

[25] X. Zhao, J. Jiang, and Z. Mao, "Effect of filter material and porosity on the energy storage capacity characteristics of diesel particulate filter thermoelectric conversion mobile energy storage system," *Energy*, vol. 283, Article ID 129068, 2023.

[26] X. Zhao, H. Zuo, and G. Jia, "Effect analysis on pressure sensitivity performance of diesel particulate filter for heavy-duty truck diesel engine by the nonlinear soot regeneration combustion pressure model," *Energy*, vol. 257, Article ID 124766, 2022.

[27] J. Xu and S. Xu, "Enhancing the interfacial bond strength of aluminum/polymer laminated film of the soft package lithium-ion battery through polydopamine surface modification," *Journal of Applied Polymer Science*, vol. 140, no. 8, 2023.

[28] Y. Chen and H. Hu, "In-plane elasticity of regular hexagonal honeycombs with three different joints: a comparative study," *Mechanics of Materials*, vol. 148, Article ID 103496, 2020.

[29] Y. Chen, N. Jiang, and H. Hu, "Mechanical modeling of an auxetic tubular braided structure: experimental and numerical analyses," *International Journal of Mechanical Sciences*, vol. 160, pp. 182–191, 2019.

[30] D. Ma, Q. Huang, Y. Wu et al., "Encapsulation of emulsions by a novel delivery system of fluid core–hard shell biopolymer particles to retard lipid oxidation," *Food & Function*, vol. 11, no. 7, pp. 5788–5798, 2020.

[31] D. Ma, Z.-C. Tu, H. Wang, Z. Zhang, and D. J. McClements, "Microgel-in-microgel biopolymer delivery systems: controlled digestion of encapsulated lipid droplets under simulated gastrointestinal conditions," *Journal of Agricultural and Food Chemistry*, vol. 66, no. 15, pp. 3930–3938, 2018.

[32] Y. Chen and M. Fu, "A novel three-dimensional auxetic lattice meta-material with enhanced stiffness," *Smart Materials and Structures*, vol. 26, no. 10, Article ID 105029, 2017.

[33] Y. Chen, B. Zheng, M. Fu, L. Lan, and W. Zhang, "Doubly unusual 3D lattice honeycomb displaying simultaneous negative and zero Poisson's ratio properties," *Smart Materials and Structures*, vol. 27, no. 4, Article ID 045003, 2018.

[34] M. Fu, Y. Chen, and L. Hu, "A novel auxetic honeycomb with enhanced in-plane stiffness and buckling strength," *Composite Structures*, vol. 160, pp. 574–585, 2017.